# A MEASUREMENT OF VA REQUIREMENTS IN AN INDUCTION TYPE BEARINGLESS MOTOR


Eichi Ito[1] Akira Chiba[1] Tadashi Fukao[2]

[1]Department of Electrical Engineering
Faculty of Science and Technology
Science University of Tokyo
2641 Yamazaki Noda Chiba Japan 278
Tel. +81(471)24-1501 Ext. 3700
Fax. +81(471)25-8651

[2]Department of Electrical and
Electronic Engineering
Tokyo Institute of Technology
Ookayama Meguro Tokyo Japan 152
Tel. +81(3)5734-2188
Fax. +81(3)5734-2903



## SUMMARY

Bearingless motors are electrical motors combined with magnetic bearing functions. In order to produce radial force, radial force windings are wound in a stator of a 4-pole induction motor. In this paper, voltage and current are measured at the radial force winding terminals of a test machine. It is found that the volt-ampere requirement is only 0.0059 times of that of the motor terminals.


## INTRODUCTION

Bearingless motors are electrical motors combined with magnetic bearing functions [1,2]. In order to produce radial force, 2-pole windings are wound in a stator of conventional 4-pole induction motors. With a current in the 2-pole windings, the 4-pole revolving magnetic field is unbalanced. Flux distributions are actively made unbalanced and the resulting radial force is effectively used for magnetic suspension of the rotor shaft. The amplitude and direction of the radial force are adjusted with negative feedback circuits employing rotor radial position detectors. In this system, one of the main concerns is how much current and voltage are required at the additional 2-pole winding terminals.

Voltage and current requirements were previously reported to be experimentally 5% of motor excitation VA by the authors [3]. However, the measured rms values were far from the theoretical values of 0.1% because of unfortunately high shaft unbalance and radial position sensors. In this paper, a test machine is built to verify the theoretical values. A shaft of the test machine is carefully balanced. It is also equipped with radial position sensors with less noise. As a result, voltage and current requirements to support its shaft are found to be only 0.0059 (0.59%) times the motor excitation VA in a test machine. Test results indicate the effectiveness of a simple theoretical calculation to estimate VA requirements of bearingless motors.

## SYSTEM CONFIGURATION AND VA REQUIREMENTS

Fig. 1 shows a system block diagram of a simple bearingless motor drive. In part of the motor controller, the motor windings are driven by a current controlled voltage source inverter which supplies sinusoidal currents with variable frequency. The amplitude of exciting current is kept constant in no-load operations. The three-phase current commands $i_{um}*$, $i_{vm}*$, and $i_{wm}*$

are generated employing the 2-phase to 3-phase transformation. Suppose the rms value of sinusoidal currents in 4-pole windings is $I_m$, then the rms line-to-line voltage of motor winding terminals $V_m$ is written, assuming sinusoidal voltage as,

$$V_m = 2\sqrt{3}\omega L_{mm} I_m \qquad (1)$$

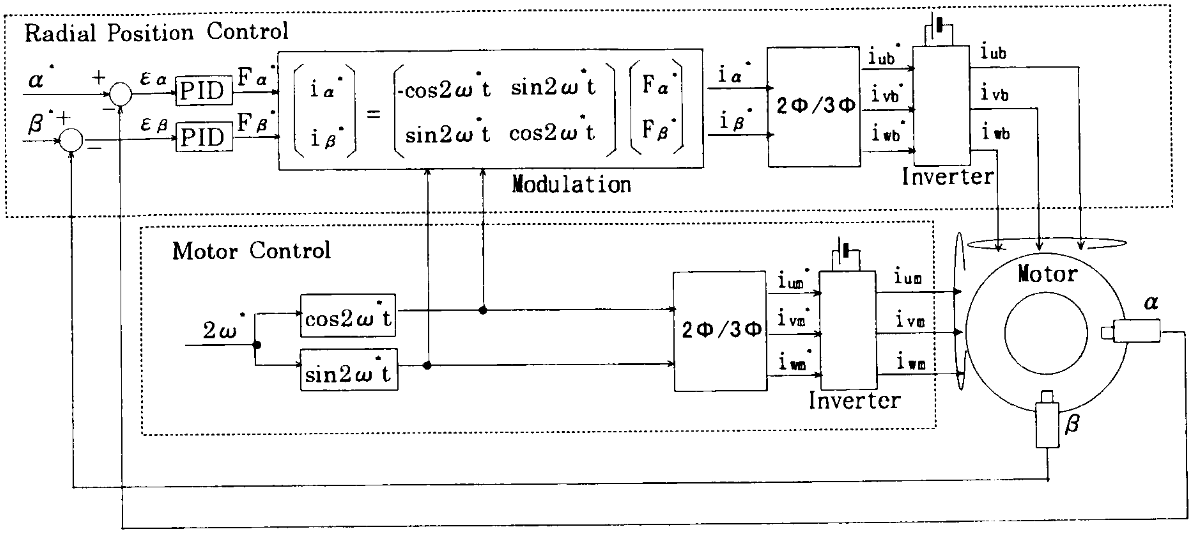


Fig. 1 System of radial position control.

where, $L_{mm}$ is a magnetizing inductance of 4-pole motor windings and $\omega$ is the mechanical angular speed of the shaft [rad/s]; and $V_m$ is proportionally increased as $\omega$ is increased. Voltage and current requirement, $VA_m$ of the 4-pole motor windings is a product of the line current and terminal voltage. Then, $Va_m$ can be defined as,

$$VA_m = \sqrt{3} V_m I_m . \qquad (2)$$

Substituting (1) into (2) yields,

$$VA_m = 6\omega L_{mm} I_m^2 . \qquad (3)$$

Note that the unit of $VA_m$ is volt-ampere [VA]. The $VA_m$ is also proportional to $\omega$.

In the radial position controller, rotor radial displacements $\alpha$ and $\beta$ are detected by radial position sensors. The detected radial positions are compared with radial position commands $\alpha^*$ and $\beta^*$, which are usually set to zero. The errors $\varepsilon_\alpha$ and $\varepsilon_\beta$ are amplified in Proportional-Integral-Differential controllers. The radial force commands $F_\alpha^*$ and $F_\beta^*$ are generated. From these radial force commands, the instantaneous current commands $I_\alpha^*$ and $I_\beta^*$ of the 2-pole radial force windings are generated with a modulation block. The inverter is controlled by the 3-phase current commands $i_{ub}^*$, $i_{vb}^*$ and $I_{wb}^*$ and supplies the currents $i_{ub}$, $i_{vb}$ and $i_{wb}$ of the radial force windings. Then radial forces corresponding to the references are generated in bearingless motors.

The rms current $I_b$ of 2-pole windings depends on the generated radial force. Let us suppose that only static radial force is generated. Thus, the current waveform is sinusoidal with angular frequency of $2\,\omega$. The relationship between radial force $F$[N] and $I_b$[A] can be written as,

$$I_b = \frac{F}{3M'I_m} \tag{4}$$

where, $M$ is a derivative of mutual inductance with respect to radial position. It is seen that if radial force $F$ is constant as in the case of the gravity force of a shaft, $I_b$ is constant. The rms value $V_b$ of fundamental line-to-line voltage at the radial force winding terminals is a product of an impedance and $I_b$. Neglecting winding resistance, $V_b$ is written as,

$$V_b = 2\sqrt{3}\omega L_{mb} I_b \tag{5}$$

where, $L_{mb}$ is magnetizing inductance. It is seen that $V_b$ is proportional to $\omega$. The voltage and current requirements of 2-pole radial force windings $Va_b$ are written as,

$$VA_b = \sqrt{3} V_b I_b . \tag{6}$$

Substituting (5) into (6) yields,

$$VA_b = 6\omega L_{mb} I_b^{\,2} . \tag{7}$$

Substituting (4) into (7) yields,

$$VA_b = 6\omega L_{mb} \left( \frac{F}{3M'I_m} \right)^2 \tag{8}$$

If $F$ is constant, $Va_b$ is proportional to $\omega$. If $\omega$ is constant and $F$ is changed, $Va_b$ is proportional to $F$ squared. $VA_m$ is also proportional to $\omega$ as seen in (3). Then, a VA Ratio $VA_b/VA_m$ is independent of rotational speed. $VA_b/VA_m$ can be obtained from the equations (3) and (6).

$$\frac{VA_b}{VA_m} = \frac{6\omega L_{mb} I_b^{\,2}}{6\omega L_{mm} I_m^{\,2}} . \tag{9}$$

Reducing (9) yields,

$$\frac{VA_b}{VA_m} = \frac{L_{mb} I_b^{\,2}}{L_{mm} I_m^{\,2}} . \tag{10}$$

If $F$ is constant, VA Ratio is constant because $I_b$ is constant from (4). If $F$ is increased, VA Ratio is proportional to $F$ squared because $VA_b$ is proportional to $F$ squared although $VA_m$ remains constant.

## CONSTRUCTION OF THE TEST MACHINE

Fig. 2 shows the cross section of a constructed test machine. Two bearingless motor units are constructed on a vertically arranged shaft. Radial positions of upper shaft end are controlled by a bearingless motor. On the other hand, thrust and radial positions in a lower shaft end are supported by a pivot bearing. Only an upper unit of bearingless motor units is tested. Radial position sensors are constructed above the upper bearingless motor unit. A touch down bearing is installed on the upper part in order to support the rotor shaft in an emergency. The air gap between rotor and touch down bearing is 100 $\mu$ m. In the bearingless motor unit, both 4-pole and 2-pole three-phase windings are wound in stator slots. The rotor has 4-pole short circuit paths to act as a 4-pole induction motor. The shaft weight including two rotors is 5.2kg.

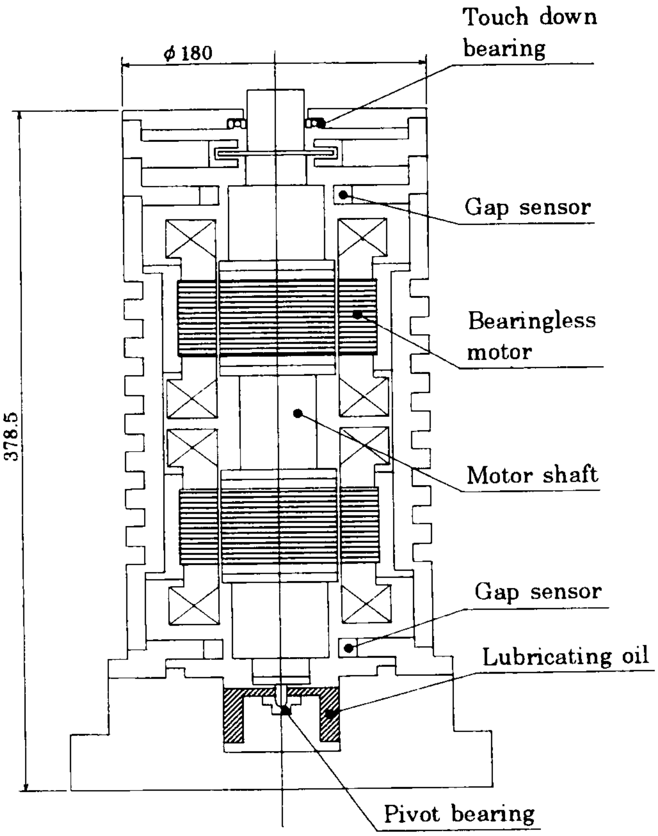


Fig. 2 Cross section of a test machine.

## A MEASUREMENT OF VA REQUIREMENTS AT 4-POLE MOTOR WINDINGS

Fig. 3 shows a system block diagram of a test system. Both 4-pole motor windings and 2-pole radial force windings are connected to voltage source inverters through digital power meters. Voltage and current rms values as well as input powers are measured. Each frequency component of current and voltage is also measured by a FFT analyzer. DC terminal voltage can be adjusted to reduce harmonics. In the 2-pole system, inductances are connected between an inverter and a digital power meter because a voltage requirement at 2-pole radial force windings is much smaller than the adjustable voltage range of the inverter. The terminal voltage was initially designed to be low enough to force line current to follow its command. As a result, the voltage is found to be fairly low. Thus, the currents follow these commands. However, DC terminal voltage can be reduced up to 20V. Thus, the voltage measurements are disturbed by harmonics. In order to avoid the undesirable harmonics, DC terminal voltage may be decreased. Thus, the inductances are connected in series.

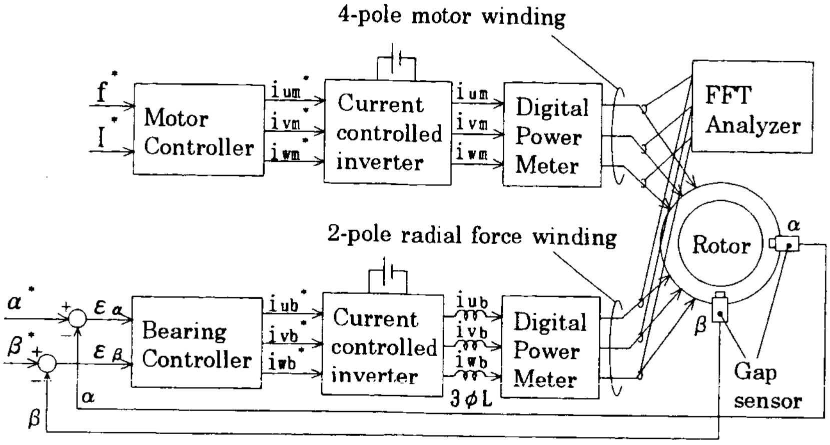


Fig. 3 The structure of the test system.

Fig. 4 shows the line currents at the 4-pole motor winding terminal. It is seen the rms values are approximately 14.0A in all speed ranges. It is also seen that fundamental components are 13.6A in all speed ranges. Note that the frequency of the fundamental components is nearly as high as twice the rotor rotational speed (2ω).

Fig. 5 shows the terminal voltage of the 4-pole motor windings. Because the rms values of terminal voltage are measured by a digital power meter, DC voltage is adjusted as small as possible to reduce harmonics while motor currents follow these commands. Although the best efforts have been made, there still remain a few harmonics. Then, measured rms voltage is slightly higher than the measured fundamental voltage. It is seen that voltages increase proportionally as rotational speed increases. Theoretical values are calculated from the equation (1). The value of magnetizing inductance of 4-pole motor windings $L_{mm}$ is shown in the Table I. These are measured from a no load test. It is seen that the rms values of terminal voltage are higher than theoretical values by about 5V because the current controlled voltage source inverter includes harmonic components.

Fig. 6 shows the voltage and current requirements at the 4-pole motor windings. The required VA can be calculated by substituting measured current values in Fig. 4 and voltage values in Fig. 5 into the equation (6). It is seen that the voltage and current requirements also increase proportionally as rotational speed increases.

Fig. 7 shows voltage and current waveforms at 10,200 r/min. It is noted that the rms value of current is about 14A and that of terminal voltage is about 26V. The voltage drop at motor winding terminals is caused by that of Insulated Gate Bipolar Transistors (IGBTs).

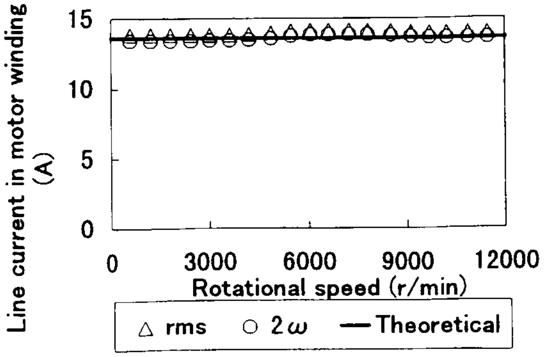


Fig.4 Current at motor windings.

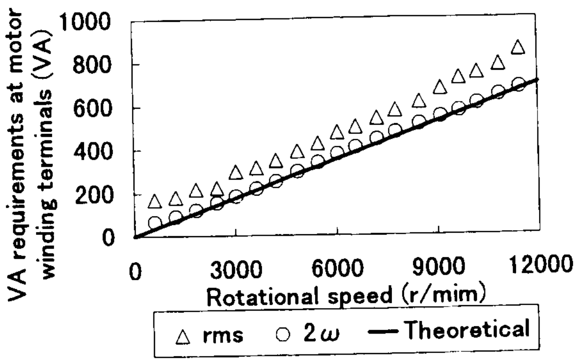


Fig.6 Voltage and current requirements at motor windings.

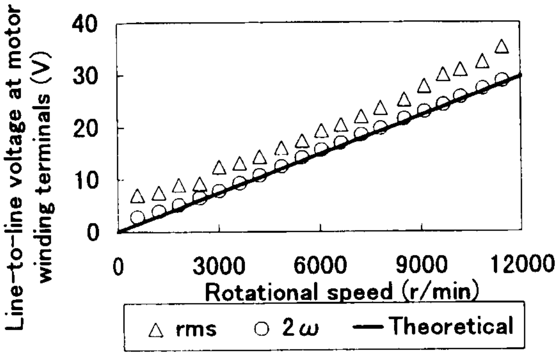


Fig.5 Terminal voltage at motor windings.

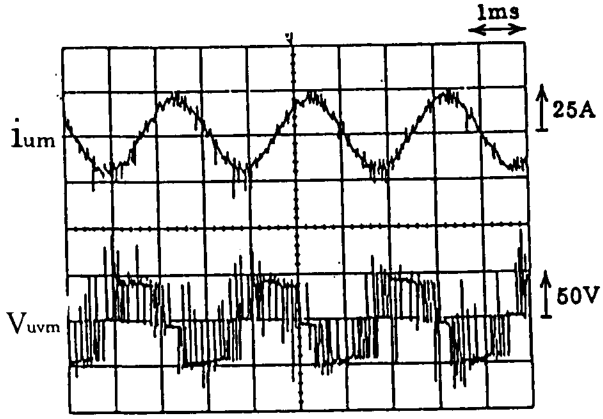


Fig.7 Waveforms at 10,200r/min.

Table I Motor parameters.

| Parameter | Values |
|---|---|
| $L_{mm}$ | 0.50(mH) |
| $L_{mb}$ | 0.38(mH) |
| M' | 0.60(H/m) |

## MEASUREMENTS OF VOLT-AMPERE REQUIREMENTS AT RADIAL FORCE WINDING TERMINALS

In the section, voltages, currents and Volt-Ampere (VA) requirements at radial force winding terminals are measured. In the voltage and current waveforms, it is suggested that values are influenced by mechanical unbalance in a certain speed range. Thus, voltage and current values are measured by a variety of equipment. Fundamental and second harmonic components of rotational frequency are measured by a FFT analyzer. Rms values are also measured by digital power meters with a wide frequency range.

As a result, it is shown that the measured second harmonic values have a good correspondence to theoretical values. The measured rms values are larger than the theoretical values. The discrepancy is mainly caused by mechanical unbalance and PWM harmonics.

### Radial force winding current with rotational and static forces

If the rotor shaft is free from radial force, any current should not flow in the 2-pole radial force windings. In practice, this is not true because there are currents caused by a negative feedback circuit. Fig. 8 shows the waveforms of radial positions $\alpha$ and $\beta$, and radial force commands $F_\alpha$* and $F_\beta$* when a static force of 2.6kgf is applied in the $\beta$-direction. When a static force is applied in the $\beta$-direction, a radial force having an amplitude which is equal to the static force is generated opposite to the $\beta$-direction. In Fig. 8, it is noted that radial positions and these commands have variations. The fundamental component of the variation is synchronized to the rotor mechanical speed. It means that radial force commands are automatically generated to suppress disturbance forces caused by the mechanical unbalance. It is also noted that $F_\beta$* contains negative DC values. This DC value is generated to produce static force. It is important to derive theoretical current representation when both static and rotational radial forces are applied to a shaft.

Let us suppose a static force $F_s$ is applied to a shaft. This force can be the weight of the rotor shaft. Let us also suppose that an amplitude of rotational radial force is $F_\omega$ which is generated by negative feedback controllers having rotational shaft displacements. The angular frequency of $F_\omega$ is exactly the same as the mechanical angular speed of the shaft. When static and rotational radial forces are applied, the radial force commands are written as,

$$F_\alpha^* = F_\omega \sin \omega t \qquad (11)$$

$$F_\beta^* = -F_s + F_\omega \cos \omega t. \qquad (12)$$

The instantaneous current command $i_\omega$* can be obtained by a modulation equation shown in a block diagram in Fig. 1, as,

$$i_\alpha^* = -F_\alpha^* \cos 2\omega t + F_\beta^* \sin 2\omega t. \qquad (13)$$

Note that the rotor speed is assumed to be exactly the same as the speed of revolving magnetic field. This assumption is valid at the no load condition. Substituting (11) and (12) into (13) yields,

$$i_\alpha^* = -F_\omega \sin \omega t \cos 2\omega t - F_s \sin 2\omega t + F_\omega \cos \omega t \sin 2\omega t. \qquad (14)$$

Let us consider the theorem of trigonometric function

$$\sin \omega t \cos 2\omega t = \frac{1}{2}(\sin 3\omega t - \sin \omega t) \qquad (15)$$

and

$$\cos \omega t \sin 2\omega t = \frac{1}{2}(\sin 3\omega t + \sin \omega t). \qquad (16)$$

Substituting (15) and (16) into (14) yields,

$$i_\alpha^* = -F_\omega \sin \omega t + F_s \sin 2\omega t. \qquad (17)$$

It is noted from equation (17) that the fundamental component of radial force winding current originates from the rotational radial force caused by mechanical unbalance. On the other hand, the second harmonic component of the current is originated from static radial force. It is also noted that the third harmonic component is canceled. These results suggest that measurements of fundamental and second components are important to see a cause of current requirements. Thus, in the following section, current is measured by a FFT analyzer to obtain amplitude of the fundamental and second harmonic components. The rms value of the current is also measured by a digital power meter.

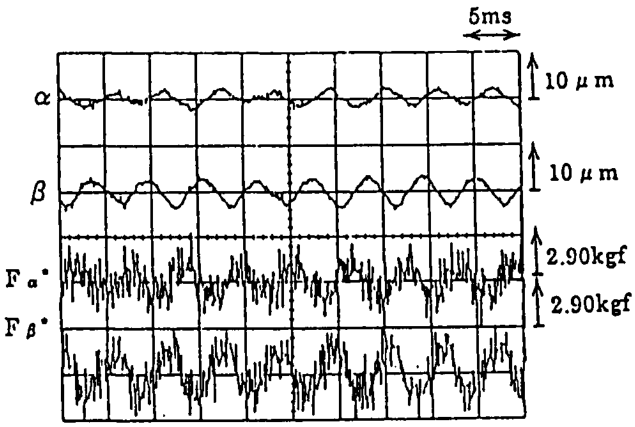


Fig. 8 Waveforms at 10,200 r/min when static force of 2.6kgf is applied.

## Voltage, current and VA requirements

Fig. 9 shows the basic experimental setup to apply radial force to the rotating shaft. A mechanical bearing is attached at the top of the shaft. Static radial force is applied through a thread connected to the mechanical bearing. The other end of the thread is connected to a weight through a pulley. Only the upper unit of the two units of a bearingless motor is used in experiments. Thus, the bottom shaft end is supported by a pivot bearing. The height of the upper unit is 219.5mm. The height of the top of the shaft is 353.0mm. Thus, radial force generated in the bearingless motor is about 1.6 times as large as the gravitational force. For example, if a weight of 1.53kg is hung, a static force of 2.6kgf is applied to the upper unit of the bearingless motor. The weight of 2.6kgf is used in this paper, because the whole shaft weighs 5.2kgf including a shaft and two bearingless rotor units.

Fig. 10 shows variations in radial force winding currents with respect to rotational speeds while a constant radial force of 2.6kgf is applied. A solid line is the theoretical value, obtained from the equation (4). The Δ plots indicate the rms values measured by a digital power meter. The □ plots indicate fundamental components (ω) measured by a FFT analyzer, which are originated by mechanical unbalance. The O plots indicate second fundamental components (2ω) measured by a FFT analyzer, which are originated from static force. The second harmonic components are nearly constant in all speed ranges as indicated by theoretical values. The second harmonic components are more dominant compared with fundamental components. The rms values are 30% ~ 40% higher than the second harmonic components because there are not only a fundamental component but also higher harmonic components. It is also seen that the fundamental component reaches the peak value at 6,000 rpm. This result indicates that a critical speed is 6,000 rpm in this machine.

Fig. 11 shows voltage variations in radial force winding terminals with respect to rotational speeds while a constant radial force of 2.6kgf is applied. A solid line is the theoretical values. The theoretical values are obtained from the equation (5). The Δ plots indicate the rms values measured by DPM. The O plots indicate second harmonic component (2 ω) measured by a FFT analyzer. The second harmonic component is increased proportionally as rotational speed increases. Good correspondence is seen between the second harmonic component and theoretical values.

However, it is seen that the rms values of terminal voltage are higher than theoretical values by about 0.5V because of the harmonics of a voltage source inverter. During the experiments, much effort has been expended to adjust DC voltage as small as possible to realize the minimum voltage requirements while the rotor does not touch down. If the DC voltage is too high, the rms value is increased because harmonics are generated by the PWM inverter. If the DC voltage is too low, the line current does not follow its command, then magnetic suspension is out of control. Thus, careful adjustments have been made in the DC voltage of the PWM inverter at every measured point. The voltage increase of 0.5V is understandable in hysteresis type current controlled PWM inverters.

Fig. 12 shows variations in radial force winding voltage and current requirements with respect to rotational speeds while a constant radial force of 2.6kgf is applied. A solid line is the theoretical values obtained from the equation (6). The Δ plots indicate the product of measured rms voltage and current. The O plots indicate the product of voltage and current of second harmonic components. The calculations of volt-ampere are based on equation (6). Thus, theoretical values are proportional to the rotational speeds. The second harmonic component corresponds to the theoretical values. The rms values are about twice as high as theoretical values at the top speed.

Fig. 13 shows variations in VA ratio with respect to rotational speeds while a constant radial force of 2.6kgf is applied. A solid line is the theoretical values obtained from the equation (9). The Δ plots are calculated from the measured rms values. The VA ratio is calculated as $VA_b/VA_m$. The $VA_m$ was previously shown in Fig. 6. The $VA_b$ is shown in Fig. 12. The O plots are calculated from the second harmonic components. VA ratio is nearly constant in all speed ranges. This fact verifies that the VA ratio is independent of rotational speed. At a speed of 10,200 rpm, VA ratio is theoretically 0.0039. In experiments, VA ratio is 0.0059 in rms values and 0.0043 in the second harmonic component values. The second harmonic value of 0.43% is close to the theoretical value. The rms value of 0.59% is 1.6 times the theoretical value. The discrepancy is caused by harmonics in voltage waveforms, mechanical unbalance, sensor noises and imperfection of controllers.

Fig. 14 shows the waveforms of radial positions $\alpha$ and $\beta$ and current at radial force winding terminals. It is seen that $i_{ub}$ contains the fundamental and second harmonic components.

Table II summarizes frequency component analysis of current and voltage at the radial force winding terminals. It is shown that the second harmonic components of current are most significant compared with other components. On the other hand, the voltage waveform contains not only the second harmonic component but also higher harmonic components because of the harmonics of a voltage source inverter.

Fig. 15 shows voltage and current waveforms at 10,200 rpm. It is seen that the voltage waveform contains significant harmonics. It is noted that the rms values of current are about 1.4A and that of terminal voltage is about 2.0V.

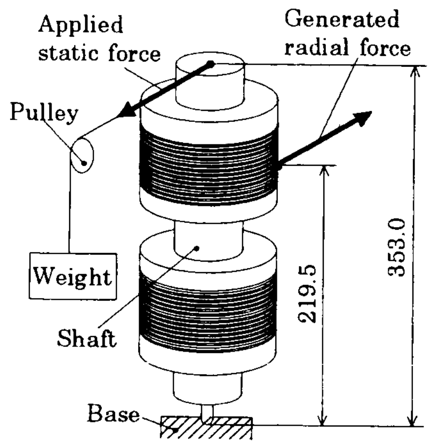


Fig.9 Mechanical radial force application.

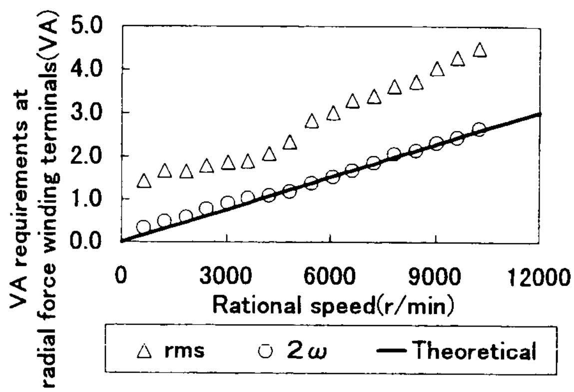


Fig.12 VA requirements at radial force winding terminals with radial force of 2.6kgf.

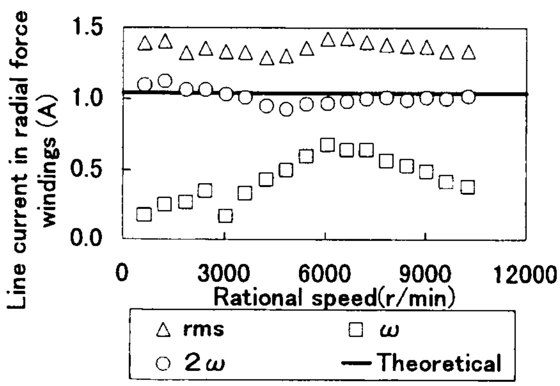


Fig.10 Line currents in radial force windings with radial force of 2.6kgf.

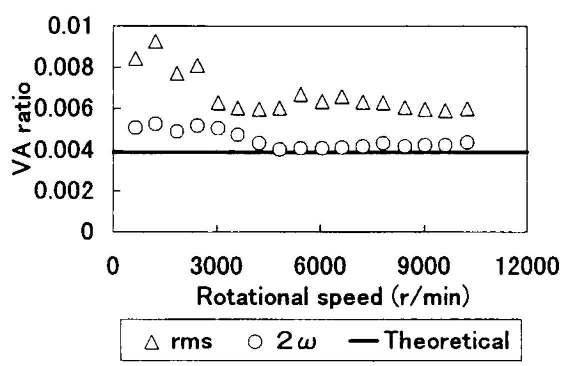


Fig.13 VA Ratio at 2.6kgf .

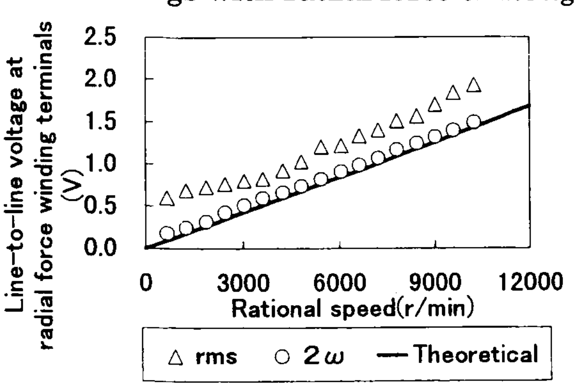


Fig.11 Line-to-line voltage at radial force winding terminals with radial force of 2.6kgf.

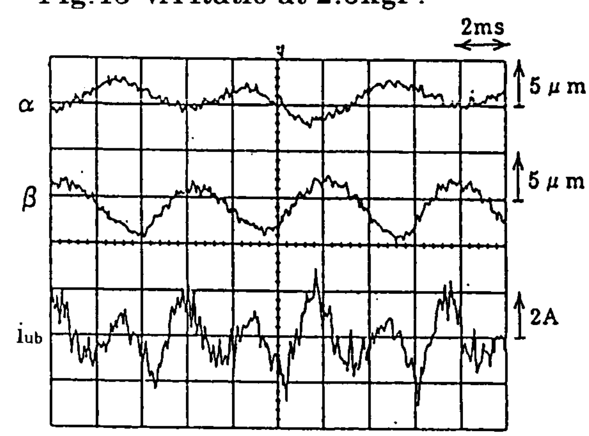


Fig.14 Waveforms at 10,200r/min when static force of 2.6kgf is applied.

Table II Frequency components at radial force winding terminals.

| Frequency component | $I_{ub}$(A) | $V_{uvb}$(V) |
|---|---|---|
| Fundmental component | 0.38 | 0.18 |
| 2 | 1.02 | 1.49 |
| 3 | 0.10 | 0.10 |
| 4 | 0.05 | 0.06 |
| 25 | - | 0.82 |
| 27 | - | 0.75 |

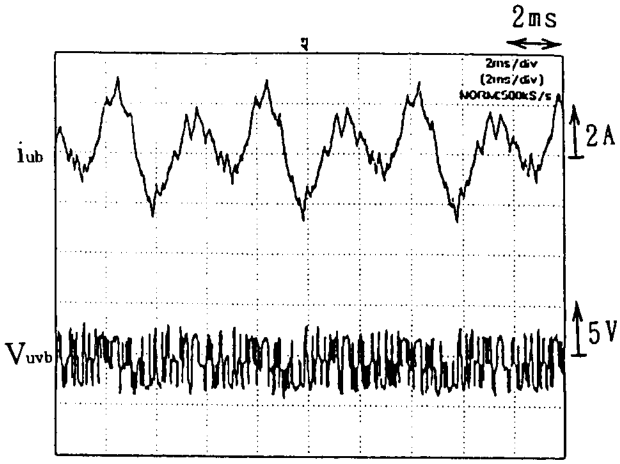


Fig.15 Waveforms at 10,200r/min when static force of 2.6kgf is applied.

Table III summarizes voltage, current, VA and VA ratio of a unit at a speed of 10,200 rpm with a radial force of 2.6kgf. Good correspondence is seen between measured second harmonic values and theoretical values. In the comparison of measured rms values and theoretical values, a good correspondence is seen only in motor winding current. A 30% increase is seen in the rms current values in radial force windings. This increase is caused by cyclic variations in shaft displacements due to mechanical shaft unbalance. The 30% increase is seen in line-to-line voltage of motor windings because of harmonics caused by PWM inverters. A 60% increase is seen in line-to-line voltage in the radial force winding terminals. One of the reasons for the increase is harmonics in a PWM inverter. The other reason is an increase of the rms current in the radial force windings. As a result, the 60% increase is seen in the VA ratio.

The index of VA ratio of 0.59%, i.e., 0.0059 can be explained employing an example. Suppose an induction motor has an output of 1.5kW. Also, suppose the exciting current of the motor is 800VA. Then, 800 x 0.0059 = 4.7VA is required to the radial force winding terminals for all three phases. If 200V line-to-line voltage is employed in an inverter, with optimization of number of turns and diameters of radial force windings, the required rms current can be derived as

$$I = 4.7 / (200\sqrt{3})$$
$$= 0.014.$$

Only 0.014A is required.

Table III
Voltage, current and VA at 10,200 r/min with 2.6kgf.

| | | Motor windings | Radial force windings |
|---|---|---|---|
| Measured 2ω component | $V_f$ | 25.7V | 1.49V |
| | $I_f$ | 13.6A | 1.0A |
| | $\sqrt{3}V_fI_f$ | 605VA | 2.6VA |
| | VA ratio | 0.43% | |
| Measured rms values | $V_{rms}$ | 31.0V | 1.94V |
| | $I_{rms}$ | 14.0A | 1.3A |
| | $\sqrt{3}V_{rms}I_{rms}$ | 752VA | 4.4VA |
| | VA ratio | 0.59% | |
| Theoretical | $V_t$ | 28.3V | 1.44V |
| | $I_t$ | 13.6A | 1.0A |
| | $\sqrt{3}V_tI_t$ | 666VA | 2.6VA |
| | VA ratio | 0.39% | |

## CONCLUSION

Voltage and current requirements were significantly higher than theoretical values in a previous paper because of unfortunately high shaft unbalance and radial position sensor noise.

In this paper, a test machine with precise mechanical balance and low noise sensors is described. The test machine was driven up to 10,200 rpm. The fundamental and second harmonic components of voltage and current were measured and the rms values of voltage and current were also measured by digital power meters. The volt-ampere (VA) requirements were also measured. The ratio of VA requirements, i.e., the VA at radial force winding terminals divided by VA at motor terminal is found to be only 0.0059.

## ACKNOWLEDGMENT

The authors wish to thank Mr. Ryoji Miyatake, who was a student in Master Course in electrical engineering in the Science University of Tokyo, for his contributions.

## REFERENCES

[1] R. Schob, and J. Bichsel: "Vector Control of the Bearingless Motor," Fourth International Symposium on Magnetic Bearings, Zurich 1994.

[2] Y. Okada, K. Dejima, and T. Oshima: "Analysis and Comparison of PM Synchronous Motor and Induction Motor Type Magnetic Bearings," IEEE Trans. IA-31, No. 5, pp. 1047-1053, 1995.

[3] Y. Takamoto, A. Chiba, and T. Fukao: "Test Results on a Prototype Bearingless Induction Motor with Five-Axis Magnetic Suspension," Proceedings of 1995 International Power Electric Conference (IPEC-Yokohama '95) Vol. 1, pp.334-339, April 7, 1995 Pacifico Yokohama.